X-RAY DIFFRACTION OF MYELIN MEMBRANE

II. Determination of the Phase Angles of the Frog Sciatic Nerve by Heavy Atom Labeling and Calculation of the Electron Density Distribution of the Membrane

C. K. AKERS *and* D. F. PARSONS

From the Biophysics Department, Roswell Park Memorial Institute, Buffalo, New York 14203

ABSTRACT The phase signs of the five main X-ray reflections from normal frog sciatic nerve have been determined as all positive using a technique of labeling with very small amounts of heavy metal. The changes in intensity of the individual reflections were studied as a function of uptake of metal label by the membrane. The possible localization of the metal label was decided from computer-analogue studies and from Patterson calculations. These phases are different from those determined by previous workers using techniques of trial of the best set of phases, or a step model, to give the best fit of the combined intensity data of normal and swollen myelin membranes. The electron density map has been calculated using eight reflections and their experimentally determined phases. The map shows an inner low electron density region which is different from that shown by earlier calculations. The center of the low electron density region shows a small region of increased electron density. However, without fixing absolute electron density levels in the map, it is not yet possible to allocate regions of low electron density to pure lipid or lipoprotein. The map shows the two sides of the membranes to be different in molecular structure without significant water spaces between the membranes.

INTRODUCTION

The radial electron density distribution (EDD) of the myelin membrane pair repeat unit can be calculated from the X-ray intensity data if the phase of each reflection is known. Because of the known method of formation of myelin membranes (Geren, 1954; Hirano and Dembitzer, 1967; Robertson, 1957) by wrapping layers of plasma membrane back to back around the axon forming a two membrane radial repeat unit, an assumption of one-dimensional centrosymmetry appears reasonable. Hence, the amplitudes are positive or negative real numbers. Finean (1962) assumed a

phase sequence of (+ + + − −) for the first five orders, but did not explain how this was derived. Subsequent workers made use of the combined intensity data for normal nerve (five main orders) and swollen nerve (up to 13 orders), and attempted to fit either a model or a set of phases so that both sets of intensity data could be satisfied. When the swollen intensity data were normalized and plotted together with the normal nerve intensity data against reciprocal space, envelopes of intensity were obtained. Finean and Burge (1963) made the assumption that the amplitude function was "well behaved" and that phases of reflections included in the same envelope had the same sign, and that adjacent envelopes alternated in sign. They arrived at a set of phases of (− + + − −). This approach had already proven to give some incorrect phases in studies of swollen hemoglobin crystals (Green, Ingram, and Perutz, 1954). Moody (1963) avoided this assumption and also the use of step-function models, and considered the fit of the mathematically-expanded normal intensity data to the swollen data when all possible (32) sets of phases were considered. This led to a final choice of two sets of phases, (− + + − −) or (− + + + +). Burge and Draper (1965) adopted an electron density step model based on the appearance of fixed and stained electron micrographs of myelin, and adjusted the model to fit the normal and swollen data. They concluded that the phases were (− + + − −). On the other hand, presumably because of the known artifacts involved in the electron microscopy of membranes (e.g., Moretz, Akers, and Parsons, 1969), Worthington and Blaurock (1968, 1969) ignored the electron microscope indications of membrane asymmetry, and chose a symmetrical model with a water space between membrane pairs. Adjustment of this model gave a fit to the envelope of swollen and normal intensity data if the phases (− + + − −) were assumed for the normal membrane structure. However, these authors (Worthington and Blaurock, 1969) point out that their X-ray data indicate that the swollen myelin membrane structure is no longer the same as the normal myelin membrane structure. In addition, it would seem an unnecessary complication, that may lead to incorrect results, to attempt to fit simple step-function models to the intensity data when only a limited number (32) of sets of phases need to be considered.

The available intensity data for myelin represents, by far, the most precise structural information yet attained for the internal organization of any membrane in a normal, physiological state. We consider it important to establish the phases with more certainty than before, so that the EDD across a pair of membranes can be calculated, and a start made towards deciding the arrangement of lipid and protein molecules inside the myelin membrane.

In this paper we report a new way of determining the phases of myelin which depends on the introduction of very small amounts of heavy metal into one major site of the membrane, without otherwise disturbing its structure or periodicity. The change in intensity of the eight recorded reflections was examined as a function of the amount of metal label taken up. The primary and secondary labeling sites

were determined by examination of the Patterson functions for normal and stained nerve, and by use of a computer analogue which tested intensity changes expected from models with various sites of metal labeling, against the observed intensity changes. The calculated EDD will be discussed in relation to other morphological and chemical composition data known about the structure of myelin.

In a later report (part III of this series) we will discuss the establishing of the absolute electron density scale of the new electron density map, and the fitting of various molecular models of myelin to the EDD.

MATERIALS AND METHODS

Grass frog (*Rana pipiens*) sciatic nerve was removed immediately after the animal was pithed. The sciatic nerve was placed in solutions (phosphate buffered saline, PBS, pH 7.2, Dulbecco and Vogt, 1954) or vapor of the heavy metal label. The nerve was then washed three times, each for 10 min, before placing it into the X-ray diffraction cell. The nerve was held in the diffraction cell under approximately 10 g of weight tension while immersed in PBS. The X-ray diffraction patterns were taken on a Kratky small angle slit camera (Kratky, 1963) at room temperature. A Siemens Crystalloflex IV X-ray generator (Siemens America, Inc., New York, N.Y.) was used at 30 kv and 30 mamp with a Kratky X-ray tube (Siemens America, Inc.) producing CuKα radiation. The camera's optimal experimental arrangement has been described in the previous publication (Akers and Parsons, 1969).

For osmium tetroxide (Fisher Scientific Company, Pittsburgh, Pa.) labeling, the vapor from a 1.5% solution (PBS, pH 7.2) was used. Ten ml of the osmium tetroxide solution was placed in the bottom of a closed container (Fig. 1). A stainless steel wire mesh was seated approximately 1 cm above the solution. The top surface of the mesh remained dry at all times. The solution was allowed to come into equilibrium with the atmosphere within the container by standing overnight in the sealed jar at 4°C. An intact frog sciatic nerve was then placed on the wire screen for the duration of the labeling time which varied from 5–25 min.

For platinic chloride ($PtCl_4$, [Fisher Scientific Company]) labeling, a 0.015% solution (PBS, pH 7.2) was used. An intact frog sciatic nerve was immersed in approximately 5 ml of solution for various labeling times (15, 30, and 60 min).

For potassium permanganate (Fisher Scientific Company), freshly prepared labeling solutions of different concentrations (0.01, 0.025, and 0.05%; PBS, pH 7.2) were used with constant labeling times of 30 min. Sequential studies on nerves labeled for different times and the relative changes in the intensities of reflections with different amounts of label were compared. This approach was greatly facilitated by the high stability of the X-ray tube

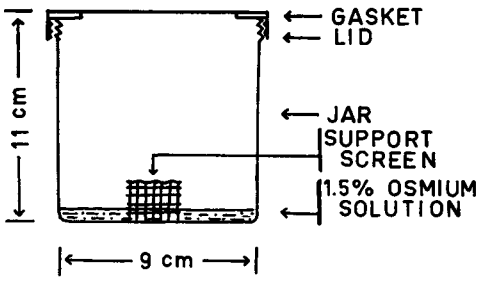

FIGURE 1 Osmium vapor labeling apparatus. Fresh intact frog sciatic nerve is placed on the support screen for various labeling times. Nerve is washed in PBS after labeling. The same apparatus is used in glutaraldehyde vapor fixation.

output as a consequence of the stabilization circuitry in the Siemens Crystalloflex IV generator. It was found that a standard scattering sample (a Lupolen sample donated by Professor O. Kratky) gave a scatter pattern reproducible in intensity to within 3% at 4.85 milliradians scatter angle.

The intensity data were used to calculate a Patterson function (Patterson, 1934) for both the unstained and the stained nerves. A computer-analogue study of the addition of electron density to the EDD simulating the addition of heavy atoms to the myelin membrane was computed (see Appendix I). Gaussian curves were used to simulate the addition of heavy atoms to the EDD. The parameters of half-width at half-height, peak height, and position of the gaussian curve were varied. Single and double labeling sites were studied using all 32 possible phase sequences. All calculations were accomplished on an IBM 1130 computer with a California Computer Products, Inc. (Anaheim, Calif.) plotter or an IBM 7040 computer.

Samples of labeled nerves were prepared for routine electron microscopy using osmium tetroxide fixation (Palade, 1952), acetone dehydration, and Epon (Shell Chemical Co., New York, N.Y.) embedding. Stained thin sections (Venable and Coggeshall, 1965) were examined to ensure that solutions of label in PBS did not cause significant disordering of the myelin structure.

The Patterson function calculations and the computer analogue indicated the principal labeled sites in the stained membrane. It was then possible to interpret the sequential change in intensities of the various reflections in terms of the phases of the reflections from the unlabeled nerve.

The phase data and the intensity were then used to calculate the electron density distribution using the Fourier transform expression developed by Blaurock and Worthington (1966).

RESULTS

Osmium tetroxide labeled sciatic nerve showed a linear increase in intensity for each of the five major reflections as heavy metal was titrated into the membrane in the initial stages of labeling (Fig. 2). However, after the initial labeling, the X-ray diffraction pattern started to change. The (200) and (400) reflections increased linearly in intensity, and then started to decrease before the (300) and (500) reflections decreased. The (100) reflection increased over the whole labeling time. The rate of increase varied from one reflection to the other, which ruled out the possibility that the heavy metal was going uniformly over the whole membrane and not to a specific site or sites of labeling. In this range of osmium uptake the periodicity of the nerve did not change. The nerve was not stiffened, but turned a smoky gray color with the addition of osmium.

The change of the intensity with osmium uptake of the weak higher order reflections (600), (800), and (1100) was also measured over the same range as gave rise to a linear intensity change for the stronger (100), (200), (300), (400), and (500) reflections. Because of their very small initial intensity (see previous paper) the intensity change was subject to more uncertainty. The (600) intensity decreased while the (800) and the (11.0.0) increased and phases of (+, +, +) respectively, were assigned to these reflections, based upon the computer-analogue calculations.

A Patterson function was calculated on the osmium labeled data (Fig. 3). After

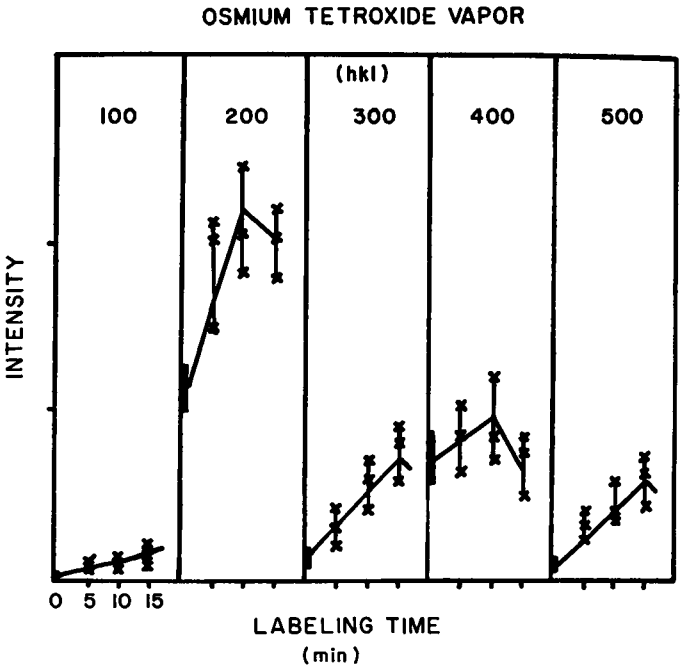

FIGURE 2 Titration curve for heavy metal osmium labeling. Fresh nerves were labeled with different amounts of osmium by placing them in the osmium vapor for different times (0–15 min). The downward trend of intensity for the (300) and (500) reflections was indicated by 20 min labeling times not included on the graph.

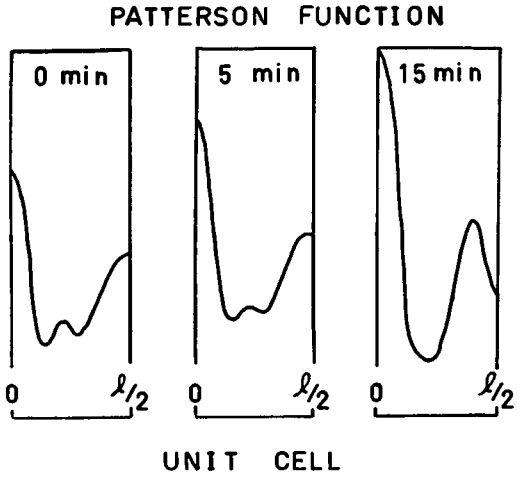

FIGURE 3 Patterson function of the osmium labeled nerve. 0, 5, and 15 min of osmium labeling are shown. The Patterson function indicates distances between scattering centers within the 171 A double membrane repeat unit. Since there is a center of symmetry only one-half a unit cell is shown.

5 min of labeling, the intensity distribution showed a considerable increase in intensity of all the reflections; yet the Patterson showed a strong peak of $l = 0$, the origin of the unit cell. There was a small broadening of the peak at $l = 0.5$. However, after 15 min of labeling time, the intensity distribution had already

changed in that the (200) and (400) reflections were starting to decrease in intensity. The Patterson function showed an additional peak which arose from scattering centers that were approximately 70 A apart. The peak is either due to another staining site or molecular rearrangement of membrane components.

The peak of the center of the membrane (*l*/4) disappeared after 15 min of labeling. This type of change in the Patterson function profile suggests that molecular rearrangement has taken place. There was also a general staining of the nerve tissue (non-myelin structure) as shown by an increase in the level of diffuse background scattering as more metal was titrated into the sciatic nerve.

Platinic chloride ($PtCl_4$) labeled sciatic nerve showed a linear increase in intensity of each reflection as more of the heavy metal was titrated into the membrane (Fig. 4). The rate of increase of each reflection also indicates that there existed a main specific staining site. There was no change in periodicity during labeling. As more metal was titrated into the nerve, it was noticed that the background scattering remained relatively constant and did not increase as the osmium tetroxide titration series increased. Thus, the platinic chloride seemed more specific on its binding than the osmium tetroxide. (A more detailed study of platinic chloride labeling of membranes will be reported separately.) The increase in the intensity of a reflection did not show discontinuities similar to those of the osmium tetroxide titration series. The nerve remained its natural color and flexible at all times.

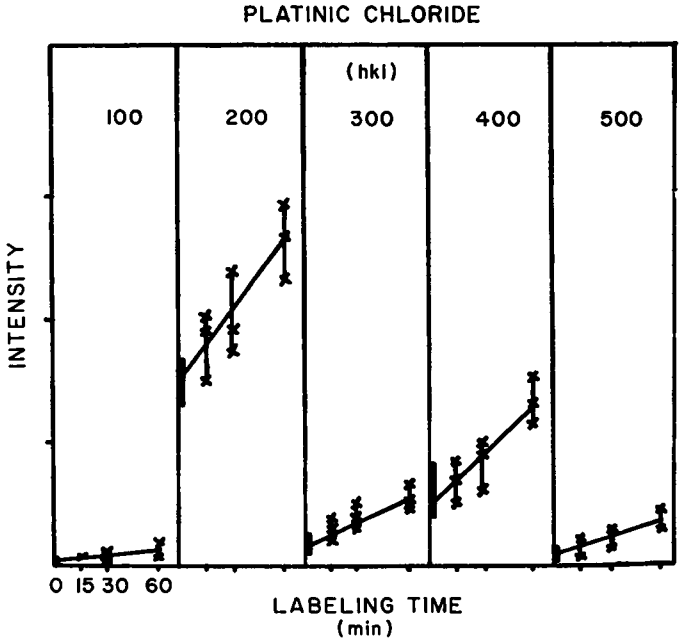

FIGURE 4 Titration curve for heavy metal labeling using platinic chloride ($PtCl_4$). Fresh nerves were placed in a 0.015% solution (PBS, pH 7.2) for different times (0–60 min). The nerve was then washed with PBS before the X-ray data was taken.

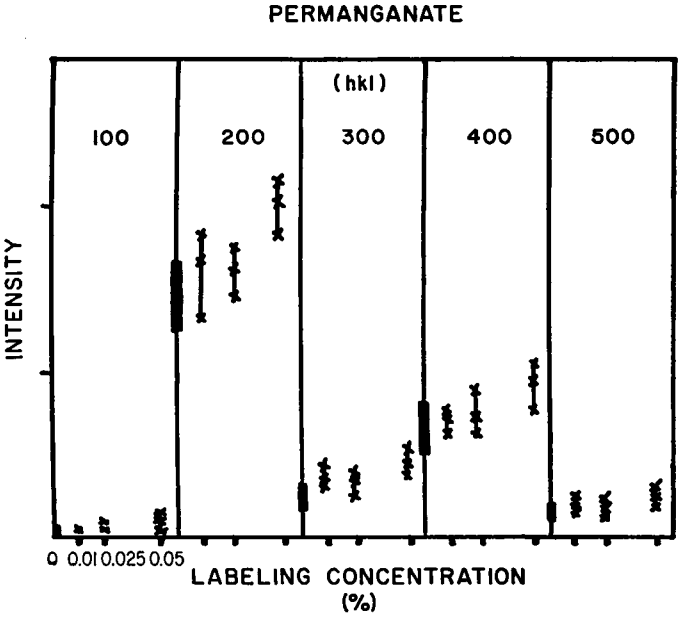

FIGURE 5 Titration curve for heavy metal labeling using potassium permanganate as the heavy metal. Fresh nerves were placed in different solutions (0.01–0.05%) for a constant amount of time. The labeled nerves were washed in PBS before the X-ray data was taken.

Potassium permanganate labeled sciatic nerve showed a linear increase in the intensity level of each reflection, but the labeling was at a slower rate (for comparable molar concentrations) than for the other heavy metals used (Fig. 5). Again, no change in periodicity occurred during labeling. The nerve tissue turned a reddish-brown color, but remained very flexible.

Other heavy metal labeling reagents which were tried included $AgNO_3$, $HgCl_2$, Hg_2Cl_2, methyl mercuric nitrate, *p*-chloromercuri-benzoic acid, bromine vapor, iodine vapor, uranyl formate, chromyl chloride, sodium tungstate, and auric chloride. These labeling reagents either caused a change in periodicity or did not react.

A computer analogue to the heavy metal labeling was computed for the five major reflections. Analysis of each of the 32 phase possibilities was accomplished by calculating the EDD for a given phase sequence, and then assuming that the contribution of heavy atoms to the EDD could be represented by the addition of electron density in the form of a gaussian function (see Appendix I). The calculated intensity of each reflection based upon the metal-modified EDD was compared to the intensities that were observed experimentally.

Three criteria were used for selecting a correct set of gaussian curve parameters. First, since the experimental data showed a positive increase in the intensity of each of the first five reflections as more metal was titrated into the membrane, the only

set of parameters that were considered were those which gave such a positive increase in the calculated intensity. Second, the order of magnitude of the increase of each reflection was chosen to agree with that of the experimental data (2nd > 4th > 3rd > 5th > 1st). Third, an R factor was defined as:

$$R = \frac{\sum_h (\Delta I\ (h00)_A - \Delta I\ (h00)_{OBS})^2}{\sum_h (\Delta I\ (h00)_{OBS})^2},$$

where $\Delta I(h00)_A$ is the change in the intensity of the (h00) reflection as the metal is titrated into the membrane according to the computer analogue. $\Delta I(h00)_{OBS}$ is the observed change in the intensity of the (h00) reflection as the metal is titrated into the membrane. R was required to be small (<5%) in order to have an acceptable fit.

A set of parameters that showed a positive increase in the intensities of all five reflections was obtained only if the phase of the (200) and (400) reflections were the same. However, the combinations (− − + + −, + − − + −, − − − + +) were exceptions from this general rule. Using a single gaussian curve of electron density, and varying the parameters of position, peak height, and half-width at half-height, did not give an acceptable fit of the calculated data to the observed data for any phase combination.

Shown in Table I are several phase sequences and their best fitting set of gaussian

TABLE I
BEST FITTING GAUSSIAN PARAMETERS FOR PHASE SEQUENCES GIVING POSITIVE INCREASES IN INTENSITIES FOR LABELED NERVE

Phase sequences	Curve I			Curve II			R
	A	$HWHH$	C	A	$HWHH$	C	
							%
− + + + +	0.2	0.03	0.0	0.2	0.03	0.45	52
+ + − + +	0.2	0.09	0.0	0.25	0.03	0.45	13
+ + + + −	0.3	0.06	0.0	0.15	0.03	0.50	22
− + + + −	0.3	0.09	0.0	0.15	0.03	0.50	55
+ + − + −	0.4	0.03	0.0	0.50	0.03	0.50	19
− + − + +	0.2	0.03	0.0	0.35	0.03	0.45	9
+ − + − −	0.10	0.06	0.0	0.15	0.09	0.50	11
− − − − +	0.25	0.09	0.0	0.1	0.03	0.5	15
+ − − − +	0.3	0.09	0.0	0.1	0.03	0.5	12
− − + − +	0.35	0.09	0.0	0.35	0.03	0.5	11
− − − + −	0.05	0.03	0.0	0.30	0.06	0.45	14
+ − − − −	0.25	0.03	0.0	0.10	0.09	0.45	9
− − + − −	0.35	0.03	0.0	0.05	0.03	0.50	10
− − − − −	0.25	0.06	0.0	0.20	0.06	0.50	8
+ + + + +	0.35	0.03	0.0	0.10	0.03	0.45	1.5

parameters. One set of parameters and phase sequence gave an acceptable fit to the observed data. The parameters of the principal gaussian curve of electron density showed a half-width at half-height of 0.03l (l = unit cell distance). This corresponds to 5 A. The position of this gaussian curve was at the origin of the unit cell (0.0l). If the highest value of electron density of the fresh, unlabeled EDD was set at 1.0, then the peak height of the curve for the principal labeling site was 0.35. The curve of the secondary labeling site of electron density was centered at 0.45l with a half-width at half-height at 0.03l. The peak height was 0.10l. Shown in Table II are several sets of parameters within the same phase sequence of (+ + + + + +). Variation of each parameter in the principal labeling site and the corresponding R factor is illustrated in the first four groups in Table II. In the last three groups of Table II, the parameters of secondary labeling sites were varied.

TABLE II

PARAMETERS OF THE GAUSSIAN CURVES OF ELECTRON DENSITY THAT SIMULATE HEAVY METAL ADDITION DURING HEAVY METAL LABELING (PHASE + + + + + +)*

Group	Curve I—Primary labeling site			Curve II—Secondary labeling site			R
	Peak height	Half-width at half-height	Position	Peak height	Half-width at half-height	Position	
							%
I	0.15	0.03	0.00	0.10	0.03	0.45	‡
	0.25	0.03	0.00	0.10	0.03	0.45	4.9
	0.35	0.03	0.00	0.10	0.03	0.45	1.5
	0.50	0.03	0.00	0.10	0.03	0.45	19.5
II	0.35	0.03	0.00	0.10	0.03	0.45	1.5
	0.35	0.06	0.00	0.10	0.03	0.45	‡
	0.35	0.09	0.00	0.10	0.03	0.45	‡
III	0.35	0.03	0.00	0.10	0.03	0.45	1.5
	0.35	0.03	0.05	0.10	0.03	0.45	‡
	0.35	0.03	0.10	0.10	0.03	0.45	‡
IV	0.15	0.06	0.00	0.10	0.03	0.45	‡
	0.35	0.06	0.00	0.10	0.03	0.45	43.3
	0.45	0.06	0.00	0.10	0.03	0.45	129.2
V	0.35	0.03	0.00	0.05	0.03	0.45	5.6
	0.35	0.03	0.00	0.10	0.03	0.45	1.5
	0.35	0.03	0.00	0.20	0.03	0.45	19.0
VI	0.35	0.03	0.00	0.10	0.03	0.45	1.5
	0.35	0.03	0.00	0.10	0.06	0.45	12.5
	0.35	0.03	0.00	0.10	0.09	0.45	46.0
VII	0.35	0.03	0.00	0.10	0.03	0.40	‡
	0.35	0.03	0.00	0.10	0.03	0.45	1.5
	0.35	0.03	0.00	0.10	0.03	0.50	5.6

* This Table illustrates how the R factor varies with variation of the gaussian parameters around the best fitting set (third line in Group I).

‡ Parameters did not produce increases in all the reflections.

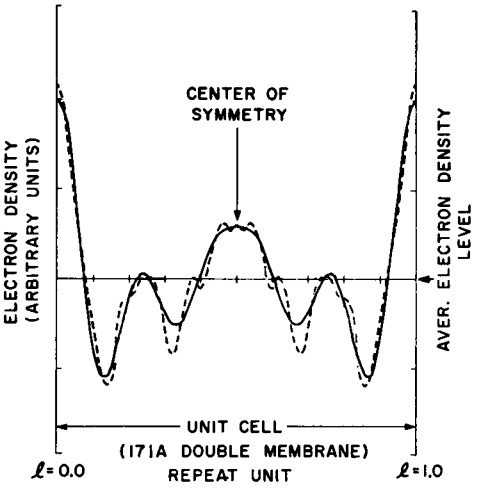

FIGURE 6 Electron density distribution (EDD) calculated with the redetermined phase signs and the appropriate Fourier transform (solid line, EDD calculated using the first five reflections; dashed line, EDD calculated using all eight reflections). The 171 A unit cell is made up of two membranes facing back to back. The membrane is asymmetric and contains a region of electron density in the center of the membrane. The dip in the central region of the membrane would be expected whether the structure is made up of lipoprotein subunits or a lipid bilayer.

As shown by Table I, and in more detail in Table II, the only set of parameters that give an acceptable agreement between the computer analogue and the observed experimental data belongs to the phase sequence of (+ + + + +).

With the correct intensities, phase information, and the appropriate Fourier transform, the EDD was calculated for the 171 A double membrane repeat unit (Fig. 6). The EDD showed that the membrane was asymmetric with a higher region of electron density on one side of the membrane, and a region of medium electron density on the other side of the membrane. In the center of the membrane there was a small region of increased electron density. When the EDD was calculated using only the five major reflections (first to fifth orders) the EDD was an undulating cosine function. The addition of the 6th, 8th, and 11th (phases determined as indicated in Appendix II) orders in the calculation of the EDD did not alter the basic electron density profile, but added detail.

At this time, no absolute electron density levels can be assigned. However, work is in progress to put the electron density map on an absolute scale. This will be reported at a later date.

DISCUSSION

In our study, as in previous studies, we have assumed that the membrane structure is centrosymmetric because the repeat unit is made up of two similar membranes placed back to back. Hence, phase angles have simply to be designated as either positive or negative.

Previous workers have used the swelling technique or model building approach to determine the phase signs of the myelin membrane (see Table III). The swelling technique involves plotting the observed amplitudes of reflections against their position in reciprocal space. The resulting plot gives a series of envelopes of am-

TABLE III
PHASE SIGN DEDUCED FOR NORMAL SCIATIC NERVE MYELIN

Investigator	Method	Phases for first five reflections
		h = 1 2 3 4 5
Finean, 1962	?	+ + + − −
Moody, 1963	Alternating signs of swelling transforms	− + + − −
Finean and Burge, 1963	Alternating signs of swelling transforms	− + + + +
		− + + − −
Burge and Draper, 1965	Phases from model based on electron microscope	− + + − −
Worthington and Blaurock, 1968	Model building to fit composite swelling transforms	− + + − −
Akers and Parsons, 1969	Metal labeling	+ + + + +

plitude. The method assumes that as the myelin swells, the EDD across the membrane is not altered, and that the membranes separate evenly. Reflections within each loop are assumed to have the same phase sign and that the loops are well-behaved functions or alternate in sign. The phase of a loop depends on the phase sign of the loop before it, which means that the phase sign of the first loop must be chosen arbitrarily. There are some serious objections to this form of the swelling method. First, the assumption that the membranes swell evenly is not justified by electron microscopy of swollen nerve. The irregular spacing of more membrane regions as seen by electron microscopy of swollen nerve probably accounts for the weak diffraction intensities obtained from swollen nerve. Second, when a loop approached zero, there was usually an uncertainty in the experimental results about whether the amplitude actually reached zero or only approached near it. Third, there were no boundary conditions that required the transform envelope to be a well-behaved function. The only boundary condition was the "principle of minimum wavelength" (Bragg and Perutz, 1952), which indicated only the minimum distance in reciprocal space that the transform envelope could change sign.

The swelling method was used in determining the phase angles in hemoglobin (Perutz, 1954), but after the phases were redetermined (Green et al, 1954) by isomorphous replacement, it was found that several phases were incorrect. Therefore, this application of the swelling technique is an uncertain one in phase determination. Finean and Burge (1963) used this technique to derive the phase information from the X-ray diffraction of the myelin membrane. With the swollen membrane data it is difficult to determine if the envelope did, in fact, go to zero or just to a minimum deflection point. The phase sequence for the first five orders as determined by the swelling method were stated to be (− + + − −). Finean and Burge (1963) arbitrarily chose the first loop to be negative so that their data would fit the Davson-Danielli bilayer theory for membrane structure (Davson and Danielli, 1943).

Other workers have made use of combined normal and swollen intensity data

without resorting to the assumptions related to the phases of the envelopes. In the approach of Worthington and Blaurock (1968, 1969) a step-function model was assumed for the normal nerve with a small water space. The water space was then expanded to generate a series of intensity or amplitude envelopes which were compared with the observed envelopes. However, this approach requires the assumption that the radial electron density distribution of the membrane pair repeat unit can be described sufficiently accurately by a model made up of a series of small steps. A step function requires many terms in the Fourier transform to describe it; whereas experimentally, we find that there are only five major reflections in the pattern and (as emphasized in the previous paper) there is no evidence that the diffraction pattern is artificially attenuated by disorder of the membrane stacks. The uniqueness of the chosen step model, with a symmetrical electron density distribution and a water space, was not established. Sufficient parameters of the model were available for adjustment of fit, and it seems possible that the good fit finally obtained with the step-function model may be, to some degree, misleading. We observed that when our undulating electron density map was converted into the closest radial step-function map, that the *R* factor or degree of fit of calculated intensities to observed intensities became poor.

The most satisfactory treatment of the combined normal and swollen intensity data appears to be that of Moody (1963). Since a limited number (32) of phase possibilities exist, Moody tested all of them without making the unnecessary assumptions involved in using a step-function model. However, in this work also, it was necessary to make the assumption that the swollen membrane was not significantly altered in structure. It is interesting that one of the two sets of phases selected by Moody (− + + + +) is similar to that determined in this study experimentally, especially when it is recognized that the first reflection, (100), is the weakest of the five and a change of sign does not greatly affect the electron density distribution.

Our method of titration of heavy metals into the membrane appears to provide an independent method for directly determining phases of intact normal nerve, which avoids the uncertainties associated with using the swollen nerve data. Of particular importance in this method is that intensity changes are studied only in situations where the labeling agent causes no change in periodicity or electron microscope indications of alterations in structure. A previous study by Millington and Finean (1958) of the effects of mercuric chloride on frog sciatic nerve did not lead to the establishing of the phase signs of the reflections, because the reagents used caused large changes in periodicity and structure of the membrane.

The observed scattering intensity of a reflection is the square of the net complex scattering amplitudes. The observed amplitude of a reflection of the labeled myelin membrane is due to the amplitude contribution of the myelin membrane times its phase factor plus the amplitude contribution of the heavy atom label times its phase factor. When the position of the heavy metal is known within the unit cell,

the phase factor of the metal's contribution to the reflection can be calculated and the phase factor of the myelin contribution can be determined.

A Patterson function was calculated from the osmium labeled data (Fig. 3). The Patterson function indicated that the metal was going mainly to a single site. However, after 15 min of labeling, the intensity profile started to change and the Patterson function showed a second scattering site appearing approximately 70 A from the primary site. This second site could be due to a secondary labeling site or to a large molecular rearrangement of the membrane. The small peak at $l/4$ in the Patterson function disappeared at large labeling times suggesting that some molecular rearrangement had taken place.

On the other hand, the computer-analogue calculations indicated that there were two sites of labeling even at small concentrations of label and before molecular rearrangement of the membrane occurred. These were a strong primary site at $l = 0.0$, in the position indicated by the Patterson and a weak secondary site at $l = 0.45$. Within the region of labeling that resulted in a linear change in intensity, we assume that the secondary labeled site is too weak to be seen on the Patterson. However, at larger times of labeling with OsO_4 a peak did appear at the secondary site indicated by the computer analogue. However, the Patterson of heavily-labeled myelin cannot be regarded as reliable since a shrinkage in the unit cell parameter has occurred and the general form of the EDD distribution (especially the disappearance of the small peak at $l = 0.25$) suggests a change in the structure of the membrane. The sign combination (+ + + + +) appears reasonable, both in terms of the Patterson function and the computer-analogue calculations.

In spite of the fact that the transform requires that the intensity be multiplied by the order (h), the weak higher order reflections, (600), (800), and (11.0.0) with phases (+, +, +) do not influence the general form of the EDD calculated from the first five strong reflections. However, they do provide interesting added detail to the density map (Appendix II) which will be considered in a report to follow, along with consideration of molecular models of the membrane that fit the absolute EDD. The behaviour of the other two labels used ($PtCl_4$ and $KMnO_4$) appeared to be the same as for the initial stages of OsO_4 labeling; and confirmed that the signs of the first five reflections were positive.

The Fourier transform which applies to the myelin membrane consists of two parts: the shape transform and the unit cell transform. The shape transform pertains to the overall shape of the myelin sheath. Due to the large radius of the myelin sheath compared to the length of the unit cell, the spiral stacking of the myelin membrane can be considered as a series of concentric cylinders. The unit cell transform pertains to the electron density distribution across the 171 A double membrane repeat unit projected onto the radial direction. The transform which applies to the electron density distribution ($t[x]$) of the myelin membrane has been developed by Blaurock and Worthington (1966), and differs significantly from that used by

Finean and Burge (1963) in that intensities are multiplied by the order index (h). (This procedure takes the Lorentz factor properly into account):

$$t(x) \propto \frac{1}{d} \sum_{1}^{+h} \pm \{h\, I(h)\}^{1/2} \cos 2\pi\, hx/d,$$

with d as the unit cell length, x as position within the unit cell ($0 \leq x \leq d$), h as the order of the reflection, $I(h)$ as the intensity of the hth order reflection.

There are some striking features about the electron density distribution across the myelin membrane. First, it can be seen that the myelin membrane is not symmetrical, but has a high electron dense side to the membrane and a less electron dense side. The difference between the two sides of the membrane probably consists of a difference in chemical nature between the two sides. Second, there exists a low electron dense region in the center of the membrane. This low level was indicated by previous workers (Finean and Burge, 1963) using other combinations of phase signs, and has been used to give support for the Davson-Danielli bilayer theory for membrane structure. However, if the membrane was made up of lipoprotein subunits (Benson, 1966), it would still have a lower electron density at the center of the membrane. This is particularly the case for a lipid-rich membrane (80% lipid by weight) such as myelin. Thus, the absolute electron density level must be determined in order to determine the composition of the material making up the low level central region of the membrane. Third, there exists a small region of medium electron density in the center of the membrane. Fourth, the electron density distribution does not contain any sharp distinct, step–function–like regions of electron density. Finally, the electron density map gives no indication of water layers between adjacent membranes, either within the unit cell or between the unit cells.

In a separate report (Moretz et al, 1969) we have closely correlated the X-ray results on myelin structure to those of electron microscopy. We have shown that a drastic change in X-ray intensity distribution occurs on dehydration in acetone or alcohol, and this is associated with loss of cholesterol and some polar lipid. The thin section method also usually gives a different periodicity to that of X-ray diffraction of the fresh nerve. This shrinkage of the unit cell is strongly suggestive of an artifactual structural change of the membrane. Various types of electron microscope preparations give single membrane thickness of from 60–93 A. We obtained for a standard Palade's OsO_4 fixed electron microscope preparation a double membrane periodicity of 133 A with a single membrane repeat of 67 A. The double membrane repeat unit for the frog sciatic nerve has been reported previously as 130–140 A (Fernandez-Moran, 1959). On the other hand, two other electron microscope techniques give periodicities more in agreement with X-ray diffraction. From negative staining of isolated beef myelin, a single membrane thickness of 87 A was seen (D. F. Parsons, unpublished). Freeze etching applied to myelin membrane (Branton, 1966; Bischoff and Moor, 1967 *a*, 1967 *b*) gave a single membrane thickness of about 93 A.

The single myelin membrane in thin section appears to be a trilaminar structure in which the peripheral surface is made up of a thin layer of weakly staining material (intraperiod line), a middle layer of nonstaining material and a thick cytoplasmic layer of densely staining material (dense line, apposed internal or cytoplasmic surfaces, [Peters, 1960; Robertson, 1958]). In spite of this striking electron microscope evidence of asymmetry, it cannot be assumed that the membrane is actually an asymmetric structure since the preparations are not free from artifacts or molecular rearrangements. The possibility that the trilaminar appearance results from the specimen preparation procedure artifacts must be considered. In our laboratory we have demonstrated that at least two types of artifacts are involved. The first occurs at the level of fixation. Cross-linking is frequently accompanied by a molecular rearrangement. This has been shown by X-ray diffraction (Moretz et al, 1969) to occur, to various degrees, with most types of fixatives used in electron microscopy. The second type of artifact indicated by our X-ray studies is associated with partial extraction of lipid during dehydration and embedding of electron microscope specimens. Many other workers (Dallum, 1957; Korn and Weisman, 1966; Morgan and Huber, 1967) have shown that a substantial lipid loss can occur subsequent to fixation. This is a specially serious matter in the case of myelin because of the unusually high lipid content of this membrane.

The freeze-etching technique is free of the artifacts associated with chemical fixatives and lipid extraction. On the other hand, the morphology may still be influenced by the glycerol (Weiss and Armstrong, 1960) used to minimize ice crystal formation, and by phase changes of the lipid associated with freezing of the membrane. The freeze-etching method applied to myelin (Branton, 1966; Bischoff and Moor, 1967 *a*, 1967 *b*) also suggests an asymmetry in the membrane. The cytoplasmic surface (staining densely in thin section preparations) shows large granular projections while the peripheral surface (staining lightly in thin section preparations) shows much finer granular projections. It is possible that the projections of opposed cytoplasmic surfaces are due to partial tearing out of the material of the adjacent membrane or contamination. It would appear likely that the coarse projections are polysaccharide because current evidence (Margolis, 1967) indicates that myelin has a low polysaccharide content.

The function of myelin, as a membrane of extra high lipid content, to act as an insulating layer around the axon surface, suggests that water would not be expected in the myelin layers. Actual evidence for the amount of water inside and adjacent to myelin membranes is sparse. It has been reported (Finean, 1957; Finean, Hawthorne, and Patterson, 1957) that 10X Ringer solution does not cause a shrinkage of the myelin membrane, but an increase of the fundamental period to 190 A. We have also observed an increase from 171–180 A with 2 N PBS. The failure to observe a decrease in the fundamental spacing suggests (but does not prove) that there is no free water between the membranes in the natural state. The possibility that myelin contains no significant thickness of water between adjacent membranes

is supported by the X-ray diffraction data of frog sciatic nerve as it slowly dries (Akers and Parsons, 1969). This indicated that the observed shrinkage (periodicity of 139 A at 16 hr of drying) occurs as a result of molecular rearrangement of the membrane structure, not loss of water.

A more certain electron microscope interpretation of the thin section appearance of myelin must await the development of fixation and embedding techniques which minimize molecular disordering and lipid extraction. Such methods are being explored in our laboratory. Finean (1957) suggested that the asymmetry indicated by X-ray diffraction is due to a "difference factor" representing a marked chemical difference between cytoplasmic and peripheral surfaces. However, the difference factor does not appear to be an essential characteristic of a myelin membrane since the myelin of optic nerve (Finean, 1960; Peters, 1960) gives a single membrane X-ray periodicity and must have only a very small difference factor in the membrane. However, electron microscopy of optic nerve usually shows a staining pattern similar to that of peripheral (sciatic nerve) only with a difference in periodicity (Finean, 1960; Hirano and Dembitzer, 1967). Sjostrand (1960) suggests that the manner in which the lipid was packed was responsible for the difference in X-ray patterns of peripheral and central nerves. This appears to be a more likely suggestion. In the electron microscope thin section preparations it is likely that the stained portions of the membrane, whether disordered or not, are associated mainly with protein rather than lipid. It is to be expected that, with present electron microscope preparation techniques, a lipid difference factor would not show up on comparing peripheral and central myelin (Napolitano, Lebaron, and Scaletti, 1967).

The possibility of cross bridges of protein stabilizing the membrane structure should be considered. Electron microscopy has shown, in a few cases (Shanthaveerappa and Bourne, 1962), structures aligned in the radial direction that could be protein bridges. Also, Napolitano et al (1967) have shown electron micrographs of the myelin membrane after it had an extraction of 98% of its lipid (peripheral nervous system contains 80% lipid and 20% protein by dry weight). The micrographs show the same "tram-line" appearance as the normal Palade's osmium-fixed, acetone-dehydrated, and Epon-embedded nerve. Since the extracted lipid must represent a large fraction of the volume of the middle part of the myelin membrane, it would appear necessary that structures such as protein cross bridges maintain the separation of the external nonlipid layers.

CONCLUSION

The phases of the X-ray diffraction amplitudes of fresh, unmodified, myelin membrane have been redetermined, by a method of heavy atom labeling, to be all real and positive for the five major reflections that relate to the 171 A double membrane radial repeating unit. The weak (600) reflection, the weak (800) reflection, and the (11.0.0) reflection are positive. The phase sequence (+ + + + +), as deter-

mined by the computer analogue, agrees with the observed changes in the intensity profile as heavy metal is titrated into the membrane. The other 31 possible phase sequences either produced negative increases in intensity or changes in the intensity profile that did not agree with the experimental data. Using the redetermined signs and the correct Fourier transform, the electron density distribution was calculated. The electron density distribution was basically an undulating cosine function (even including the detail introduced by the 6th, 8th, and 11th reflections), and confirmed that most of the lipid must be located in the central region of the membrane. Absolute electron density levels cannot yet be assigned to the map, and so the choice between bilayer and lipoprotein models cannot yet be made. However, the map indicates that the two surfaces are different and that no significant water layer exists between adjacent membranes.

We thank Dr. A. Guinier, University of Paris, and Dr. W. J. Walbesser, State University of New York at Buffalo, for their advice, Roger Moretz and Ali Hamad for assistance with the electron microscope.

This work was, in part, supported by National Science Foundation Grant GB-7130, American Cancer Society Grant E-457 and Grant IN54H-6.

Received for publication 25 June 1969 and in revised form 4 August 1969.

APPENDIX I

Simulation of the Heavy Atom Labeling Experiments by Computer Analysis

Electron density, due to the addition of heavy atom labeling being titrated into the membrane, was represented by a gaussian curve:

$$\text{Electron density } (x) = A \cdot \text{EXP } (-B \cdot [x - C]^2),$$

where A equals peak height; B equals constant which is a function of half-width at half-height ($HWHH$); C equals the peak center position along the x axis. The parameters A, B, and C were varied in this analysis. Due to a center of symmetry, for a peak to be at C, there must also exist a similar peak at $(l - C)$ with l equal to unit cell parameter. The position of the guassian curve, C, was varied in steps of $0.05l$. The half-width at half-height was varied in steps of $0.03l$. The constant, B, equals $\ln(\frac{1}{2})/HWHH^2$. The peak height was varied in steps of 0.05 g the maximum, with the maximum equal to the maximum electron density value of the EDD of the normal nonlabeled myelin.

Double labeling sites were investigated by varying A, B, and C for each gaussian curve. The EDD was calculated using one of the 32 possible phase sequences. The gaussian curves of electron density, simulating the heavy atom, were added to the normal nonlabeled EDD. The intensity profile for the modified EDD was calculated and compared to that of the nonlabeled EDD. The changes in the intensity profile were then compared to those which were observed experimentally after 10 min of labeling.

The degree of correlation, between the analogue calculations and the observed experimental data, was determined by three criteria: (*a*) the intensity profile must show a positive increase when the gaussian curves of electron density were added to the normal EDD; (*b*)

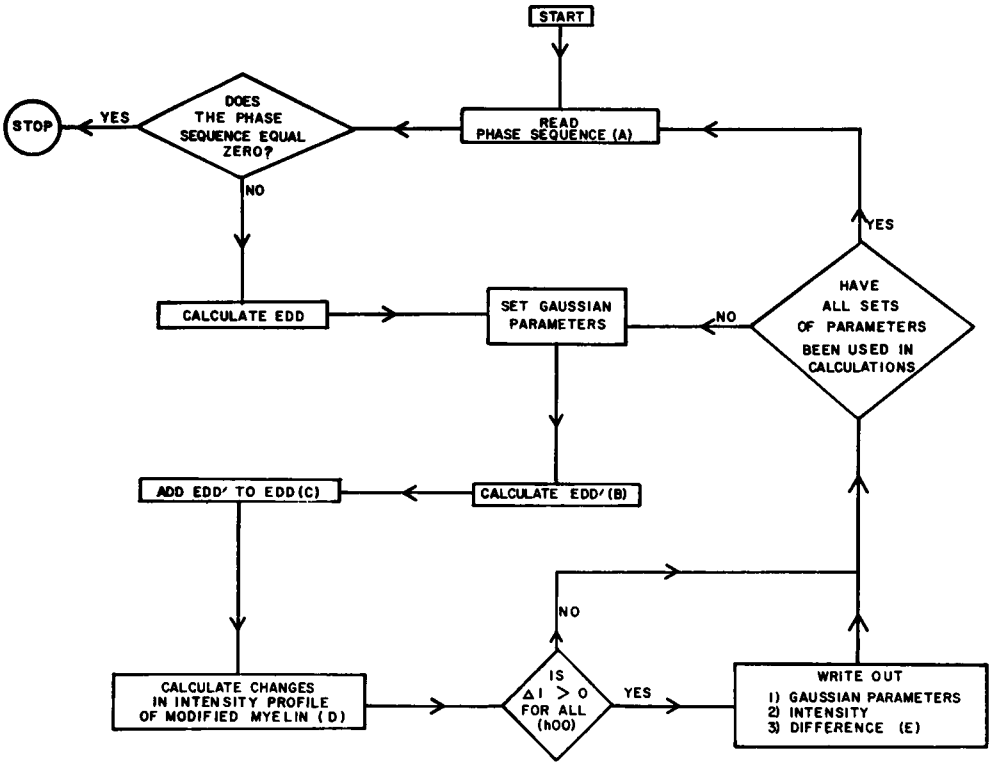

FIGURE 7 Flow chart of computer analogue. *A*, all 32 possible phase sequences were used; *B*, EDD of heavy atom label simulated by gaussian curve; *C*, labeled EDD; *D*, ΔI equals intensity of labeled myelin minus intensity of nonlabeled myelin; *E*, difference ΔI (analogue) minus ΔI (observed).

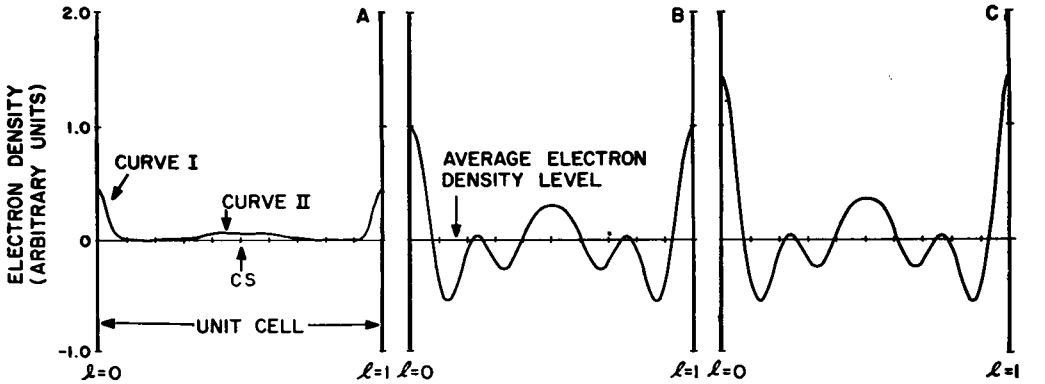

FIGURE 8 Graphical example of computer analogue. *A*, EDD due to two heavy metal labeling sites simulated by gaussian curves at $l = 0.0$ and 0.45 (CS is center of symmetry); *B*, normal unlabeled EDD of the myelin membrane (calculated only with the five major reflections; *C*, the EDD of the labeled myelin membrane (sum of the EDD in 8 *A* and 8 *B*).

the order of the intensity of the reflection must be identical to the observed order; and (*c*) the *R* factor must be small (1.5%).

The flow chart of the computer program used is shown in Fig. 7. Fig. 8 is an example of a computer analogue. In Fig. 8 *A*, the two sites of labeling (curve I and curve II) are shown and their corresponding curves which are determined by the center of symmetry. The parameters of curve I are $A = 0.45\ H$, $B = 0.03l$, and $C = 0.00l$, where H is the maximum value of the normal, unstained EDD. In Fig. 8 *B*, one sees the normal EDD of the nonlabeled myelin membrane using the phase sequence of (+ + + + +) to which the EDD from Fig. 8 *A* is added. The intensity profile calculated from the modified EDD (Fig. 8 *C*) is compared to that of the nonlabeled EDD. The changes in the intensity profile are then compared to the experimental data as the heavy atom is titrated into the myelin membrane.

The total computing time on the IBM 1130 computer was approximately 125 hr.

APPENDIX II

Effect of the Phase of the 6th, 8th, and 11th Order Reflections on the EDD

The phases of the (600), (800), and (11.0.0) reflections were determined as follows. The best fitting metal electron density distribution, determined as described in Appendix I,

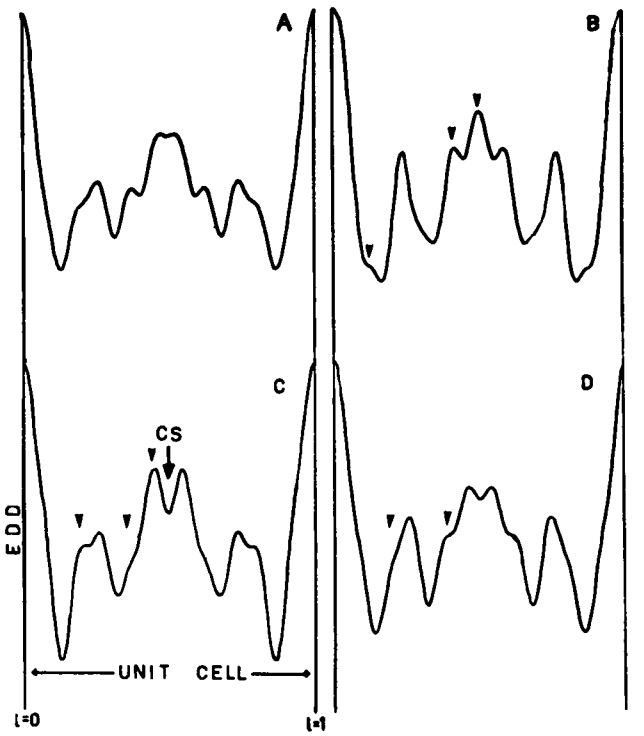

FIGURE 9 The effect of the phase sign of the 6th, 8th, and 11th order reflections (EDD = electron density distribution; CS = center of symmetry). *A*, phase sequence of + + +; *B*, phase sequence of − + −; *C*, phase sequence of − − +; *D*, phase sequence of − + +.

for the five main reflections was used to calculate the sign of the phase of the metal contribution to the (600), (800), and (11.0.0) reflections. This was carried out by using the Blaurock and Worthington transform expression. The phase sign of the metal contribution was found to be (− + +). Since short-term metal labeling caused the intensity of the (600) reflection to decrease, and the (800) and (11.0.0) reflections to increase, the phase sign of the myelin contribution to these reflections must be (+ + +) for the 6th, 8th, and 11th orders respectively.

The sign sequence (+ + +) for the amplitudes of the 6th, 8th, and 11th order reflections produce an EDD as shown in Fig. 9 *A*. If the sign sequence was (− + −) for the 6th, 8th, and 11th order reflections (Fig. 9 *B*), then the calculated EDD showed new peaks of density at 0.14*l* and 0.50*l* (*l* = unit cell distance) with a disappearance of the peak at 0.37*l* in Fig. 9 *A*. The peak at 0.47*l* was shifted to 0.42*l* and the peak at 0.18*l* disappeared. If the sign sequence was (− − +) for the 6th, 8th, and 11th order reflections then the calculated EDD showed an enhancement of the peak at 0.18*l* which also shifted to 0.20*l*. The peak at 0.37*l* decreased while the peak at 0.45*l* increased (Fig. 9 *C*). If the sign sequence was (− + +) (Fig. 9 *D*) for the 6th, 8th, and 11th order reflections, then the calculated EDD showed enhancement of peaks of density at 0.37*l* and a decrease of the peak at 0.20*l*.

The EDD was determined to be in the form of an undulating cosine function when only the five major reflections were used in the calculation. The addition of the 6th, 8th, and 11th order reflections did not basically change the EDD, but only added detail. The sign of the 11th order reflection appears to have the greatest effect upon the EDD detail, while the sign of the 6th order has the least effect upon the EDD detail.

REFERENCES

AKERS, C. K., and D. F. PARSONS. 1969. *Biophys. J.* **10**:101.

BENSON, A. A. 1966. *J. Amer. Oil Chem. Soc.* **43**:265.

BISCHOFF, A., and H. MOOR. 1967 *a. Z. Zellforsch.* **81**:303.

BISCHOFF, A., and H. MOOR. 1967 *b. Z. Zellforsch.* **81**:571.

BLAUROCK, A. E., and C. R. WORTHINGTON. 1966. *Biophys. J.* **6**:305.

BRAGG, L., and M. F. PERUTZ. 1952. *Roy. Soc. London Proc.* **213A**:425.

BRANTON, D. 1966. *Exp. Cell Res.* **45**:203.

BURGE, R. E., and J. C. DRAPER. 1965. *Lab. Invest.* **14**:978.

DALLUM, R. D. 1957. *J. Histochem. Cytochem.* **5**:178.

DAVSON, H., and J. F. DANIELLI. 1943. The Permeability of Natural Membranes. Cambridge University Press, London.

DULBECCO, R., and M. VOGT. 1954. *J. Exp. Med.* **99**:167.

FERNANDEZ-MORAN, H. 1959. *Rev. Mod. Phys.* **31**:319.

FINEAN, J. B. 1957. *In* Metabolism of the Nervous System. D. Richer, editor. Pergamon Press, New York. 52.

FINEAN, J. B. 1960. *In* Modern Scientific Aspects of Neurology. J. N. Cumings, editor. E. Arnold Ltd., London. 232.

FINEAN, J. B. 1962. *Circulation.* **26**:1151.

FINEAN, J. B., and R. E. BURGE. 1963. *J. Mol. Biol.* **7**:672.

FINEAN, J. B., J. N. HAWTHORNE, and J. D. E. PATTERSON. 1957. *J. Neurochem.* **1**:256.

GEREN, B. B. 1954. *Exp. Cell Res.* **7**:558.

GREEN, D. W., V. M. INGRAM, and M. F. PERUTZ. 1954. *Roy. Soc. London Proc.* **225A**:287.

HIRANO, A., and H. M. DEMBITZER. 1967. *J. Cell Biol.* **34**:555.

KRATKY, O. 1963. *Prog. Biophys. Mol. Biol.* **13**:105.

KORN, E. D., and R. A. WEISMAN. 1966. *Biochim. Biophys. Acta.* **116**:309.

MARGOLIS, R. 1967. *Biochim. Biophys. Acta.* **141**:91.

MILLINGTON, P. F., and J. B. FINEAN. 1958. *J. Ultrastruct. Res.* **2**:215.

MOODY, M. F. 1963. *Science (Washington)*. **142**:1173.
MORETZ, R., C. K. AKERS, and D. F. PARSONS. 1969. *Biochim. Biophys. Acta*. **193**:1, 12.
MORGAN, T. E., and G. C. HUBER. 1967. *J. Cell Biol.* **32**:757.
NAPOLITANO, L., F. LEBARON, and J. SCALETTI. 1967. *J. Cell Biol.* **34**:817.
PALADE, G. E. 1952. *J. Exp. Med.* **95**:285.
PATTERSON, A. I. 1934. *Phys. Rev.* **46**:372.
PERUTZ, M. F. 1954. *Roy. Soc. London Proc.* **225A**:264.
PETERS, A. 1960. *J. Biophys. Biochem. Cytol.* **7**:121.
ROBERTSON, J. D. 1957. *J. Biophys. Biochem. Cytol.* **3**:1043.
ROBERTSON, J. D. 1958. *J. Biophys. Biochem. Cytol.* **4**:349.
SHANTHAVEERAPPA, T. R., and G. M. BOURNE. 1962. *Nature (London)*. **196**:1215.
SJOSTRAND, F. S. 1960. *In* Modern Scientific Aspects of Neurology. J. N. Cumings, editor. E. Arnold Ltd., London. 188.
VENABLE, J. H., and R. COGGESHALL. 1965. *J. Cell Biol.* **25**:407.
WEISS, L., and J. A. ARMSTRONG. 1960. *J. Biophys. Biochem. Cytol.* **7**:673.
WORTHINGTON, C. R., and A. E. BLAUROCK. 1968. *Nature (London)* **218**:87.
WORTHINGTON, C. R., and A. E. BLAUROCK. 1969. *Biochim. Biophys. Acta*. **173**:427.